RSC Advances

This is an *Accepted Manuscript*, which has been through the Royal Society of Chemistry peer review process and has been accepted for publication.

Accepted Manuscripts are published online shortly after acceptance, before technical editing, formatting and proof reading. Using this free service, authors can make their results available to the community, in citable form, before we publish the edited article. This *Accepted Manuscript* will be replaced by the edited, formatted and paginated article as soon as this is available.

You can find more information about *Accepted Manuscripts* in the Information for Authors.

Please note that technical editing may introduce minor changes to the text and/or graphics, which may alter content. The journal's standard Terms & Conditions and the Ethical guidelines still apply. In no event shall the Royal Society of Chemistry be held responsible for any errors or omissions in this *Accepted Manuscript* or any consequences arising from the use of any information it contains.

ROYAL SOCIETY OF CHEMISTRY

www.rsc.org/advances

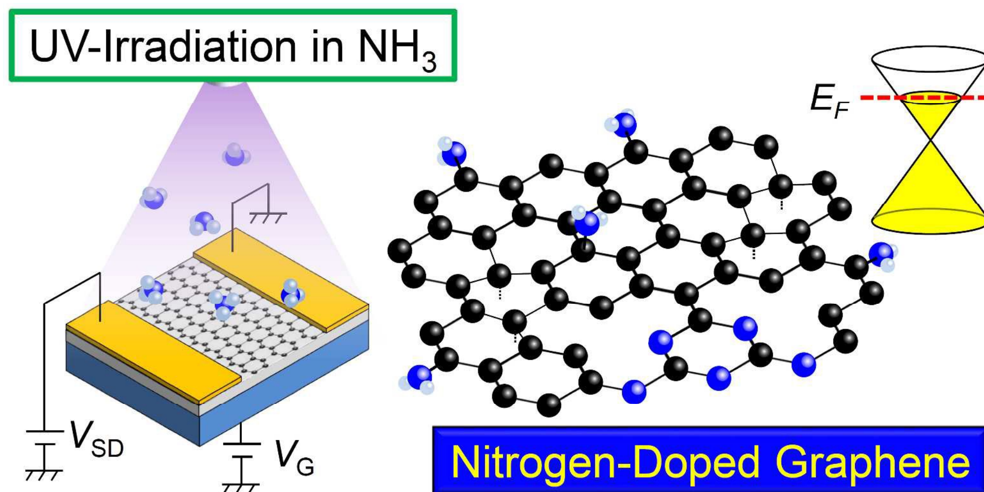

Control of electron concentration in graphene is achieved in the range of 10^{12} - 10^{13} cm^{-2} by nitrogen doping using photochemical reactions.
415x207mm (192 x 192 DPI)

RSC Advances Accepted Manuscript

RSC Advances

ARTICLE

Effect of UV light-induced nitrogen doping on the field effect transistor characteristics of graphene

Received 00th January 20xx,
Accepted 00th January 20xx

DOI: 10.1039/x0xx00000x

www.rsc.org/

Gaku Imamura*[ab] and Koichiro Saiki[b]

The effect of nitrogen doping to graphene was characterized without exposing the prepared specimen to atmosphere. Nitrogen doping was done via photochemical process at room temperature, in which graphene on SiO_2/Si was irradiated by UV light in ammonia. Field effect transistor measurements revealed that the UV-irradiation to graphene in NH_3 causes electron doping of ~10^{12} cm^{-2} (~0.01%) as a result of N-doping, which can be controlled by changing the irradiation time. Comparing the transfer characteristics and the Raman spectra, we discuss the structure of the graphene functionalized via photochemical reactions, and the corresponding electronic structure.

Introduction

Graphene, one atom thick sheet of sp^2 carbon atoms arranged in a honeycomb configuration, has been intensively studied as a novel 2D material in recent years. Its prominent mechanical, electronic, chemical properties make graphene a key material for next-generation technologies.[1,2] Doping to graphene with heteroatoms is one of the most promising methods for modifying its properties[3]. It is reported that nitrogen (N) doping gives rise to the evolution of a band gap[4,5]. The opening the band gap leads to a high on/off ratio, which is essential for application to electronic devices. Another interesting phenomenon evoked by N-doping is the catalytic activity for oxygen reduction reaction[6], the cathode reaction of fuel cells. Carbon alloy catalysts (CACs), the assembly of N-doped graphene, can be seen as an inexpensive alternative to platinum[7,8]. With regard to CACs, increased conductivity by electron doping as a result of N-doping is important rather than emergence of a band gap. Despite the many studies on the synthesis of N-doped graphene[9-17], controlling the doping level is still a big challenge. One of the major reasons is the trade-off relationship between the degree of graphenization and the N-doping amount; the former requires a high growth temperature, while the latter decreases rapidly with temperature[13-17]. To overcome such a dilemma, a N-doping method effective still at room temperature is required. In addition, a direct N-doping method to graphene that can control the doping level has been highly anticipated. Most of past studies using chemical vapour deposition (CVD) needed a transfer process for characterization, which made it difficult to deduce the intrinsic nature of doping due to the inevitable subsidiary effect.

In our previous study, we succeeded in fabricating N-doped graphene by exposing the graphene to NH_3 atmosphere under UV light irradiation[18]. This method enables us to characterize the electrical properties before and after N-doping *in situ*. In the present study, we have observed a shift of the charge neutrality point (CNP) to the negative direction after the UV-irradiation in NH_3, which indicates electron doping to graphene. The doping levels can be controlled in the range of 10^{12} - 10^{13} cm^{-2} by varying the irradiation time. On the basis of transport measurements and Raman spectroscopy, we discuss the possible structure for the N-doped graphene.

Experimental

There are several methods to fabricate graphene such as mechanical exfoliation of graphite, epitaxial growth on SiC, reduction of graphene oxide, and CVD process including solid

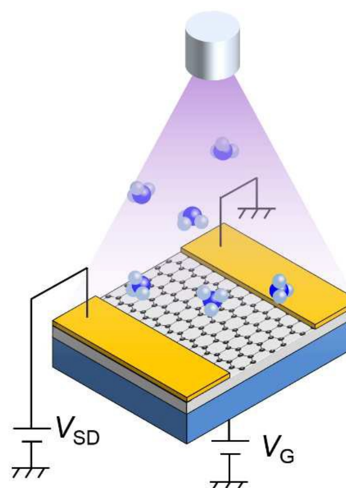

Figure 1. Schematic illustration of the experimental setup.

[a] World Premier International (WPI) Research Center, International Center for Materials Nanoarchitectonics (MANA), National Institute for Materials Science (NIMS), 1-1 Namiki, Tsukuba, Ibaraki 305-0044, Japan. Tel: +81-29-851-3354 (ext. 4186). Fax: +81-29-860-4706. E-mail: IMAMURA.Gaku@nims.go.jp
[b] Department of Complexity Science and Engineering, Graduate School of Frontier Sciences, The University of Tokyo, Kashiwanoha 5-1-5, Kashiwa, Chiba 277-8561, Japan.

† Electronic Supplementary Information (ESI) available: See DOI: 10.1039/x0xx00000x

This journal is © The Royal Society of Chemistry 20xx

RSC Advances Accepted Manuscript

Please do not adjust margins

carbon sources[19-25]. To ensure the quality and uniformity of graphene on SiO_2, we purchased graphenes on SiO_2(285 nm)/Si from Graphene Laboratories Inc., which were fabricated via CVD process. The specimens were taken from the same lot. Figure 1 shows a schematic illustration of the experimental setup. To fabricate a field effect transistor (FET) structure, 20-nm-thick gold pads were deposited onto the graphene as source and drain electrodes. After wiring the electrodes to vacuum feedthroughs, the chamber was evacuated to ~10^{-6} Pa. Electrical measurements and UV-irradiation were performed in the vacuum chamber. Prior to electrical measurements, the graphene was annealed in a vacuum at 160 °C for several hours, which removed adsorbed molecules and contaminants. Ammonia was introduced into the chamber via a variable leak valve. A deuterium lamp (L2D2, 30 W, Hamamatsu Photonics K.K.) was used for UV-irradiation. The peak emission wavelength of the lamp is around 150-200 nm, and the effective power density is estimated to ~0.01 mW/cm^2. Raman spectroscopy was performed in air with excitation wavelength of 532 nm.

Results and Discussion

Figure 2a shows the FET characteristics of the graphene before and after UV-irradiation in NH_3. Typical transfer characteristics of

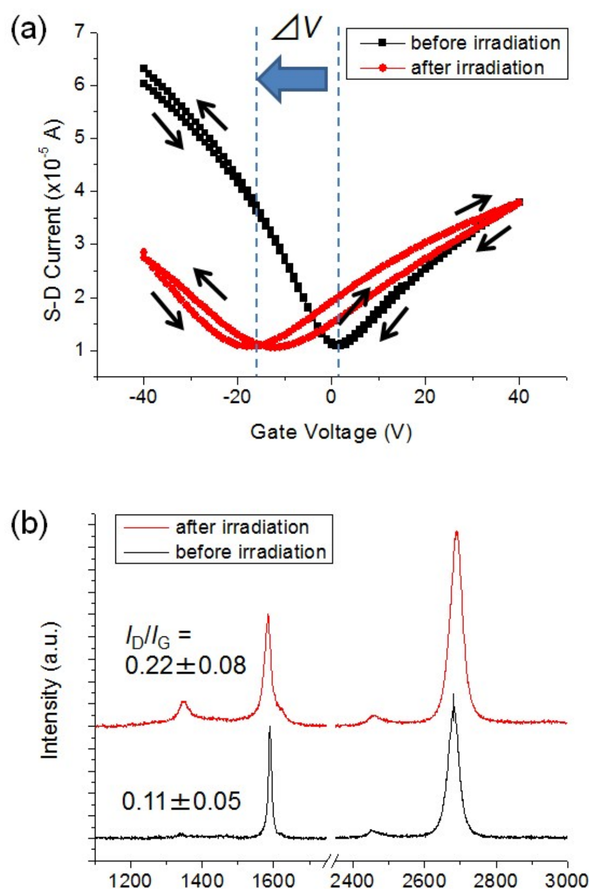

Figure 2. (a)Transfer characteristics of graphene before and after the UV-irradiation in NH_3. (b) Raman spectra of graphene before and after the UV-irradiation in NH_3.

pristine graphene could be observed before the UV-irradiation[26]; CNP was located at around 0 V, and the curve exhibited a small hysteresis. The carrier mobility of the graphene was 1,100 cm^2/(V s) and 2,300 cm^2/(V s) for electron and hole transport, respectively. After the FET measurement, the graphene was UV-irradiated under 10 Pa of NH_3 for 1 h at RT. The evolution of a hysteresis and the decrease of mobility was observed after the UV-irradiation (Fig. 2a). For the forward sweep (from a negative to a positive gate voltage), the electron mobility (μ_e) and hole mobility (μ_h) decreased to 720 cm^2/(V s) and 1,200 cm^2/(V s), respectively. μ_e and μ_h for the backward sweep (from a positive to a negative gate voltage) were 790 cm^2/(V s) and 940 cm^2/(V s), respectively. The evolution of a hysteresis and the decrease of mobility were explained by the formation of sp^3-like bonds at the graphene/SiO_2 interface as described in Ref. 27. Our previous study showed that UV-irradiation in a vacuum triggers a photochemical reaction at the graphene/SiO_2 interface, which gives rise to the decrease in mobility and the hysteresis that was counter clockwise on the negative side and clockwise on the positive side. Another noticeable change in FET characteristics after the UV-irradiation in NH_3 was a shift in the CNP to the negative direction. The CNP is shifted by –16 V after the UV-irradiation in NH_3, while UV-irradiation in a vacuum does not shift the CNP[27]. Hence, it is implied that the CNP is shifted to the negative direction as a result of N-doping, by which nitrogen atoms are incorporated into the graphene lattice. Incorporation of N atoms by UV irradiation in ammonia was confirmed by X-ray photoelectron spectroscopy in our previous study[18].

Figure 2b shows the Raman spectra of the graphene before and after the UV-irradiation in NH_3. Three inherent peaks for graphene are seen for both spectra: the G band (~1585 cm^{-1}), the D band (~1,350 cm^{-1}), and the 2D band (~2,700 cm^{-1})[28]. The D band originating from the A_{1g} vibrational mode of hexagonal sp^2 carbon network becomes Raman active by defects. Therefore, the intensity ratio of the D band to the G band (I_D/I_G) is a good indicator for evaluating the density of defects[29,30]. While the pristine graphene showed small I_D/I_G (0.11±0.05), the graphene UV-irradiated in NH_3 exhibited higher I_D/I_G (0.22±0.08). Thus defects were introduced into the graphene lattice by the UV-irradiation in NH_3. As the sharp symmetric 2D band was not substantially changed after irradiation, the structure of monolayer graphene remained.[31] The widening of the 2D band reflects the defect formation in graphene[32,33].

RSC Advances Accepted Manuscript

This journal is © The Royal Society of Chemistry 20xx

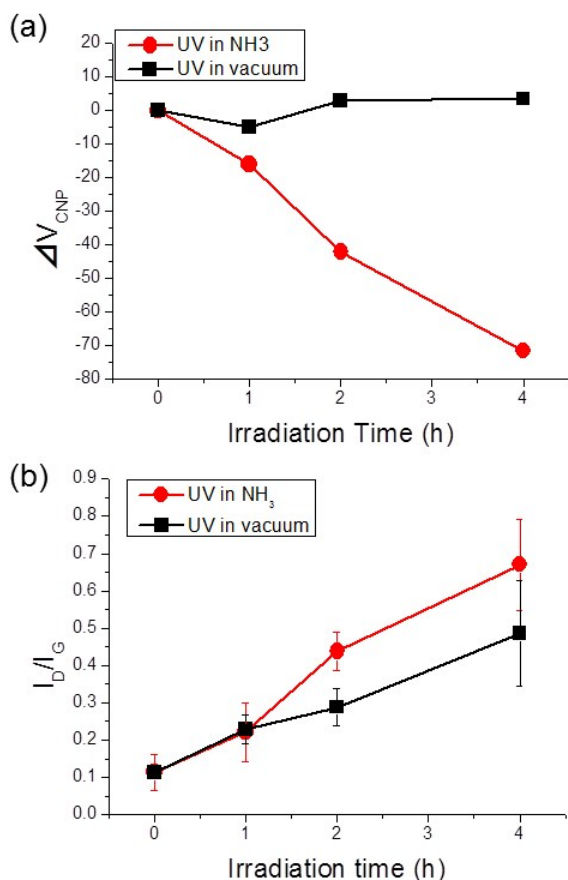

Figure 3. (a)ΔV_{CNP} as a function of irradiation time. (b) Raman I_D/I_G as a function of irradiation time.

To investigate the dependence on the irradiation time, graphene was UV-irradiated in 10 Pa of NH_3 for longer times (2 h and 4 h). The shift in CNP (ΔV_{CNP}) was plotted as a function of irradiation time in Fig. 3a. ΔV_{CNP} is almost proportional to the irradiation time. We estimate the doped electron density (n_e) from ΔV_{CNP} according to the capacitor relationship: $n_e = C_{ox}\Delta V_{CNP}/e$, where C_{ox} and e are the capacitance of SiO_2 per area and the elementary charge, respectively. n_e for the graphene UV-irradiated in NH_3 for 1 h, 2 h, and 4 h is estimated to 1.3×10^{12} cm^{-2}, 3.4×10^{12} cm^{-2}, 6.1×10^{12} cm^{-2} , respectively. Considered that the atomic number density of graphene is 3.8×10^{15} cm^{-2}, the corresponding doping level for the graphene UV-irradiated in NH_3 for 1 h, 2 h, and 4 h is 0.034 %, 0.089 %, and 0.16 %, respectively. Thus the electron density of graphene can be controlled in the range of 10^{12} - 10^{13} cm^{-2} (0.01 %) by the UV-irradiation in NH_3. With regard to carrier mobility, the changes in electron and hole mobility (μ_e and μ_h, respectively) are summarised in table 1.

Table 1. Mobility and charge neutrality point for each sample.

Irradiation time		μ_e (cm^2/Vs)	μ_h (cm^2/Vs)	V_{CNP} (V)
1 h	Before	1,000	2,300	1
	After (- → +)	720	1,200	-18
	After (+ → -)	790	940	-12
2 h	Before	1,500	1,800	2
	After (- → +)	710	790	-41
	After (+ → -)	770	640	-38
4 h	Before	1,200	1,600	3
	After (- → +)	510	-[a]	-73
	After (+ → -)	500	-[a]	-70

[a] Mobility cannot be calculated because gate voltage more negative than 80 V could not be applied to prevent dielectric breakdown.

To elucidate the relation between the N-doping and the formation of sp^3-like bonds by the UV-irradiation, we compared the results with the data from the graphene UV-irradiated in a vacuum[27]. With regard to the FET characteristics, the CNP is shifted to the negative side after UV-irradiation in NH_3, while the CNP stays

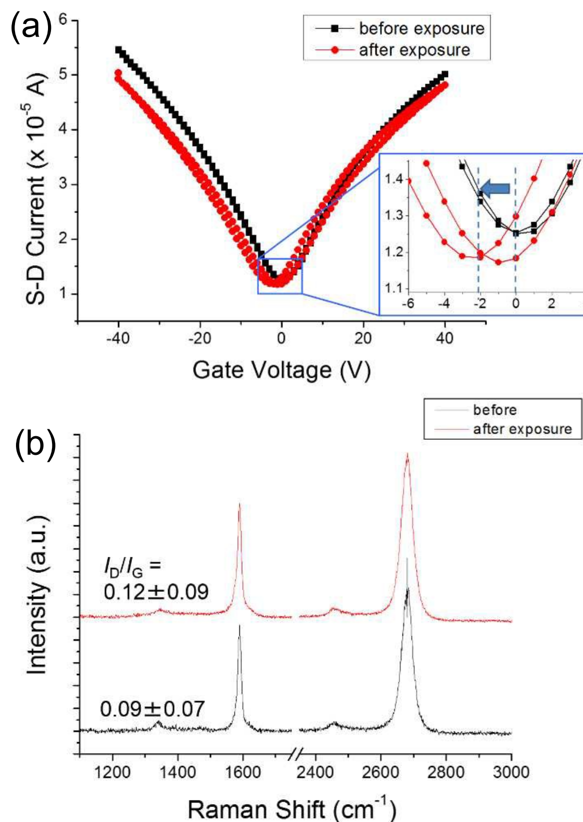

Figure 4. (a)Transfer characteristics of graphene before and after exposure to NH_3. (inset) Enlarged transfer characteristics at around the Dirac point. (b) Raman spectra of graphene before and after exposure to NH_3.

RSC Advances Accepted Manuscript

Please do not adjust margins

at around 0 V for the graphene UV-irradiated in a vacuum (Fig. 3a). The difference between NH_3 and vacuum can also be seen in the change of Raman spectra as shown in Figure 3b. While the I_D/I_G monotonically increased with irradiation time for both conditions, the degree of increase is larger for the UV-irradiation in NH_3 than that in a vacuum. This higher I_D/I_G implies that graphene is damaged by N-doping as well as the formation of sp^3-like bonds caused by UV-light.

The effect of adsorption of ammonia on graphene was also studied by exposing the graphene on SiO_2/Si to 10 Pa of NH_3 for 1h without UV-light. Figure 4a shows the FET characteristics before and after the exposure. No noticeable change can be observed after the UV-irradiation without a small shift of CNP to the negative direction. Such small negative shift after the exposure to NH_3 has also been reported by Romero *et al.*, which is considered to be caused by displacement chemical reactions in the graphene/SiO_2 interface[34]. The Raman spectra also showed no changes at all. (Fig. 4b)

On the basis of the experimental results, we propose a possible structure of N-doped graphene together with the electronic structure in Fig. 5. Before the UV-irradiation in NH_3, the Fermi level was located at the Dirac point judging from the V_{CNP} of around 0 V (Fig. 2a). The shift of the CNP after the UV-irradiation in NH_3 indicated that electrons were doped into graphene, and the Fermi level was shifted to higher energy. It is known that UV light induces a photodissociation reaction of NH_3 molecules described as

$$NH_3 \rightarrow NH_2 + H,$$

which yields active NH_2 radicals[35]. As the activation energy for this reaction is 6.0 eV (corresponding to photon with a wavelength of 206 nm), the deuterium lamp used in this study can induce this reaction. By means of chemical reactions between such NH_2 radicals and graphene, we have reported that graphene is functionalized with amino groups as well as the formation of g-C_3N_4 domains[18]. Several studies have reported that amino groups would act as an electron donor for graphene[36,37], hence the amino groups introduced via the photochemical reaction are responsible for the electron doping. In addition to the amino groups and g-C_3N_4 domains, sp^3-like bonds are also formed at the graphene/SiO_2 interface[18,27], which are responsible for the decrease in the carrier mobility and the hysteresis behaviour. Such undesirable defects may be reduced by indirect UV irradiation in ammonia, by which the graphene sample is not directly UV-irradiated.

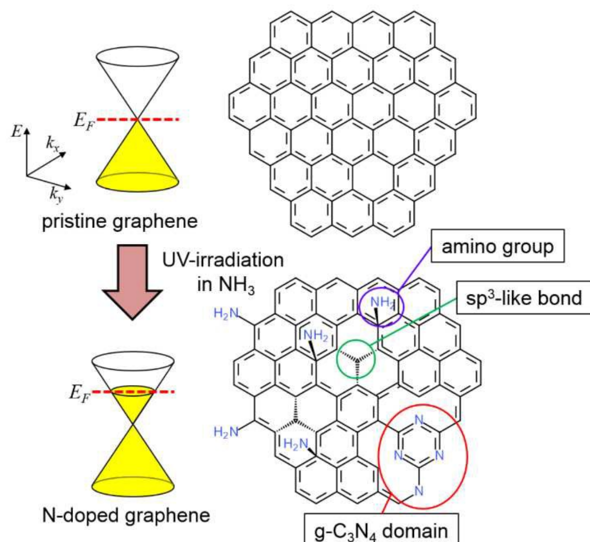

Figure 5. Schematic illustration of N-doped graphene and the corresponding electronic structure.

The density of defects (σ_d) can be estimated from the Raman I_D/I_G. According to the Tuinstra-Koenig relation, the average crystalline size (L_a) is described as $L_a = C/(I_D/I_G)$, where C is a constant depending on the excitation wavelength. (C = 19.2 for 532 nm)[29,30,38] As L_a is the average distance between the defects, σ_d is written as $\sigma_d = 1/L_a^2 = (I_D/I_G)^2/C^2$. Note that any structural disorders including vacancies, sp^3 carbon structures, and doped impurities contribute to σ_d in this estimation. As I_D/I_G was 0.22±0.08 for the graphene UV-irradiated in NH_3 for 1 h, σ_d is estimated to be 1.26×10^{10} cm^{-2}, which is approximately 1/100 of the doped electron density (n_e) estimated from the shift of the CNP (1.3×10^{12} cm^{-2}). This significant deviation implies that defect formation including N-doping occurs rather locally. The estimation of σ_d assumes randomly distributed defects in graphene. Therefore σ_d is likely to be underestimated if defects are locally formed. It is highly plausible that defects are localized in some regions of graphene. Formation of g-C_3N_4 domains is one of such examples. As we have discussed in the previous study, x-ray photoelectron spectroscopy implies that g-C_3N_4 domains are formed in the graphene lattice[18]. Another case is that defects such as amino groups or sp^3-like bond are localized at the periphery of graphene grains. As it is known that graphene is more reactive at grain boundaries than at a centre of domains[39-41], defect formation is likely to occur at the periphery of domains.

Another explanation for the smaller defect density is the fact that defect density can be underestimated for the UV-induced defects. The studies on estimation of L_a or σ_d from the Raman I_D/I_G are based on the physically induced defects caused by ion-bombardment. However, I_D/I_G should depends on the types of defects[42]. On the basis of the phenomenological model[30], we conclude that both sp^3-like bonds and amino groups give rise to lower I_D/I_G than the structural disorders caused by ion-bombardment, resulting in the smaller defect density. The details are provided in the supporting information.

Conclusions

Graphene on a SiO_2/Si substrate was irradiated by UV-light in NH_3 at room temperature, and its FET characteristics were measured before and after the irradiation *in situ*. The electrical measurement has revealed that the electrons are doped via N-doping. By means of UV-irradiation in NH_3, we have demonstrated that electron doping level can be controlled in the range of 10^{12} - 10^{13} cm^{-2} (0.01%). The FET measurements and the Raman spectroscopy indicate that N atoms are doped as amino groups and g-C_3N_4 domains, and defects including N-containing species are formed rather locally. This study shows a possibility of N-doping via UV-irradiation, and provide a new strategy to modify the electronic properties of graphene.

RSC Advances Accepted Manuscript

 This journal is © The Royal Society of Chemistry 20xx

Acknowledgements

This work was supported by the New Energy and Industrial Technology Development Organization (NEDO) and also by a Grant-in-Aid for Scientific Research from MEXT of Japan (No. 25107002).

Notes and references

1 K. S. Novoselov, V. I. Fal'ko, L. Colombo, P. R. Gellert, M. G. Schwab, K. Kim, *Nature*, 2012, **490**, 192−200.
2 H. Choi, S. Jung, J. Seo, D. W. Chang, L. Dai, J. Baek, *Nano Energy*, 2012, **1**, 534−551.
3 H. Liu, Y. Liu, D. Zhu, *J. Mater. Chem.*, 2011, **21**, 3335–3345.
4 A. Lherbier, A. Rafael B. Méndez, J.C. Charlier, *Nano Lett.*, 2013, **13**, 1446–1450.
5 D. Usachov, O. Vilkov, A. Grüneis, D. Haberer, A. Fedorov, V. K. Adamchuk, A. B. Preobrajenski, P. Dudin, A. Barinov, M. Oehzelt, C. Laubschat, D. V. Vyalikh, *Nano Lett.*, 2011, **11**, 5401–5407.
6 Z. Yang, H. Nie, X. Chen, X. Chen, S. Huang, *J. Power Sources,* 2013, **236**, 238−249.
7 T. Ikeda, M. Boero, S. Huang, K. Terakura, M. Oshima, J. Ozaki, *J. Phys. Chem. C*, 2008, **112**, 14706–14709.
8 G. Chai, Z. Hou, D. Shu, T. Ikeda, K. Terakura, *J. Am. Chem. Soc.*, 2014, **136**, 13629−13640.
9 X. Wang, X. Li, L. Zhang, Y. Yoon, P.K. Weber, H. Wang, J. Guo, H. Dai, *Science,* 2009, **8**, 768-771.
10 D. Wei, Y. Liu, Y. Wang, H. Zhang, L. Huang, G. Yu, *Nano Lett.*, 2009, **9**, 1752–1758.
11 D. Long, W. Li, L. Ling, J. Miyawaki, I. Mochida, S. Yoon, *Langmuir*, 2010, **26**, 16096–16102.
12 C. Zhang, L. Fu, N. Liu, M. Liu, Y. Wang, Z. Liu, *Adv. Mater.*, 2011, **23**, 1020–1024.
13 G. Imamura, K. Saiki, *J. Phys. Chem. C*, 2011, **115**, 10000–10005 (2011).
14 G. Imamura, C. Chang, Y. Nabae, M. Kakimoto, S. Miyata, and K. Saiki, *J. Phys. Chem. C,* 2012, **116**, 16305–16310.
15 T. Katoh, G. Imamura, S. Obata, M. Bhanuchandra, G. Copley, H. Yorimitsu, K. Saiki, *Phys. Chem. Chem. Phys.,* 2015, **17**, 14115–14121.
16 T. Terasawa, K. Saiki, *Jpn. J. Appl. Phys.,* 2012, **51**, 055101.
17 T. Katoh, G. Imamura, S. Obata, K. Saiki, submitted to *Carbon*.
18 G. Imamura, K. Saiki, *Chem. Phys. Lett.,* 2013, **587**, 56–60.
19 M. Cai, D. Thorpe, D.H. Adamson, H.C. Schniepp, *J. Mater. Chem.* 2012, **22**, 24992-25002.
20 W. Norimatsu, M. Kusunoki, Phys. Chem. Chem. Phys., 2014, **16**, 3501-3511.
21 F. Perrozzi, S. Prezioso, L. Ottaviano, *J. Phys.: Condens. Matter* 2015, **27**, 013002.
22 Y. Zhang, L. Zhang, C. Zhou, *Acc. Chem. Res.*, 2013, **46**, 2329–2339.
23 Z. Sun, Z. Yan, J. Yao, E. Beitler, Y. Zhu, J.M. Tour, *Nature* 2010, **468**, 549-552.
24 A.K. Kesarwani, O.S. Panwar, S. Chockalingam, A. Bisht, S.R. Dhakate, B.P. Singh, A.K. Srivastava, R.K. Rakshit, *Sci. Adv. Mater.* 2014, **6**, 2124-2133.
25 O.S. Panwar, A.K. Kesarwani, S.R. Dhakate, B.P. Singh, R.K. Rakshit, A. Bisht, S. Chockalingam, *J. Vac. Sci. Technol. B* 2013, **31**, 040602.
26 F. Schwierz, *Nat. Nanotechnol.*, 2010, **5**, 487–496.
27 G. Imamura, K. Saiki, *ACS Appl. Mater. Interfaces*, 2015, **7**, 2439–2443.
28 L.M. Malard, M.A. Pimenta, G. Dresselhaus, M.S. Dresselhaus, *Physics Reports*, 473, 51–87 (2009)
29 A. C. Ferrari, J. Robertson, *Phys. Rev. B*, 2000, **61**, 14095.
30 M.M. Lucchese, F. Stavale, E.H.M. Ferreira, C. Vilani, M.V.O. Moutinho, R.B. Capaz, C.A. Achete, A. Jorio, *Carbon*, 2010, **48**, 1592−1597.
31 A.C. Ferrari, J.C. Meyer, V. Scardaci, C. Casiraghi, M. Lazzeri, F. Mauri, S. Piscanec, D. Jiang, K.S. Novoselov, S. Roth, A.K. Geim, *Phys. Rev. Lett.* 2006, **97**, 187401.
32 D.C. Kim, D.-Y. Jeon, H.-J. Chung, Y.S. Woo, J.K. Shin, S. Seo, Nanotechnology 2009, **20**, 375703.
33 L. Liu, S. Ryu, M.R. Tomasik, E. Stolyarova, N. Jung, M.S. Hybertsen, M.L. Steigerwald, L.E. Brus, G.W. Flynn, *Nano Lett.* 2008, **8**, 1965-1970.
34 H.E. Romero, P. Joshi, A.K. Gupta, H.R. Gutierrez, M.W. Cole, S.A. Tadigadapa, P.C. Eklund, *Nanotechnology*, 2009, **20**, 245501.
35 J. Biesner, L. Schnieder, G. Ahlers, X. Xie, K.H. Welge, *J. Chem. Phys.*, 1989, **91**, 2901–2911.
36 F. Liu, N. Tang, T. Tang, Y. Liu, Q. Feng, W. Zhong, Y. Du, *Appl. Phys. Lett.,* 2015, **106**, 013110.
37 I. Lee, H. Park, J. Park, J. Lee, W. Jung, H. Yu, S. Kim, G. Kim, J. Park, *Org. Electron.*, 2013, **14**, 1586–1590.
38 F. Tuinstra, J.L. Koenig, *J. Chem. Phys.,* 1970, **53**, 1126−1130.
39 D. Jiang, B.G. Sumpter, S. Dai, *J. Chem. Phys.* 2007, **126**, 134701.
40 R. Sharma , J.H. Baik , C.J. Perera, M.S. Strano, *Nano Lett.*, 2010, **10**, 398–405.
41 N. Mitoma, R. Nouchi, *Appl. Phys. Lett.* 2013, **103**, 201605.
42 S. Niyogi, E. Bekyarova, M.E. Itkis, H. Zhang, K. Shepperd, J. Hicks, M. Sprinkle, C. Berger, C.N. Lau, W.A. deHeer, E.H. Conrad, R.C. Haddon, *Nano Lett.*, 2010, **10**, 4061–4066.

RSC Advances Accepted Manuscript